Measurements of Nonlinear Growth of Ion-Acoustic Waves in Two-Ion-Species Plasmas with Thomson Scattering

D. H. Froula,* L. Divol, and S. H. Glenzer

L-399, Lawrence Livermore National Laboratory, University of California, P.O. Box 808, Livermore, California, 94551

(Received 16 October 2001; revised manuscript received 6 February 2002; published 25 February 2002)

We report the first Thomson-scattering measurements of the growth of ion-acoustic waves in well-characterized multi-ion-species plasmas consisting of gold and beryllium. We observe that only the berylliumlike mode grows, verifying linear kinetic theory. In addition, a twofold increase in ion temperature is measured when ion-acoustic waves are excited to large amplitudes by stimulated Brillouin scattering (SBS). This increase in ion temperature is a strong indication of hot ions due to trapping. We explain the measured SBS reflectivity by nonlinear detuning of the SBS instability due to these trapping effects.

DOI: 10.1103/PhysRevLett.88.105003 PACS numbers: 52.25.Os, 52.35.Fp, 52.38.–r, 52.50.Jm

Indirect drive inertial confinement fusion depends on efficient propagation of high intensity laser beams through multi-ion-species plasmas in closed-geometry hohlraums. Understanding ion-wave growth and the saturation mechanisms in these plasmas is necessary to improve the energy coupling in the fusion capsule and to develop models that will predict stimulated Brillouin scattering (SBS) laser energy losses at future fusion facilities such as the National Ignition Facility. The SBS instability results from the resonant coupling of an intense laser pulse with an ion-acoustic wave. The resulting driven ion-acoustic wave has been shown to saturate [1–4]. A possible mechanism to explain ion-wave saturation is frequency detuning by trapping [1,5].

In this Letter, we present the first observations of the growth of ion-acoustic waves in a well-characterized multi-ion-species plasma consisting of Au and Be. Using Thomson scattering, we directly measure the growth of the ion-acoustic wave responsible for the SBS light. The temporally resolved Thomson-scattering spectra show simultaneously the scattering from thermal ion-acoustic fluctuations and ion-acoustic waves that have been excited to large amplitude by SBS using a 2ω interaction beam. For this experiment, the solution to the kinetic dispersion relation gives slow and fast ion-acoustic modes which are evident in our Thomson-scattering spectra as fast Be-like and slow Au-like peaks [6]. We observe that only the Be-like mode grows, verifying predictions made by linear kinetic theory. In addition, we use a new technique that measures the relative damping of the slow and fast modes to determine the ion temperature with high accuracy. We measure up to a factor of 2 increase in the ion temperature when ion-acoustic waves are excited by SBS. This measurement of the ion temperature, and its correlation with SBS, is the first direct quantitative evidence of hot ions created by trapping in laser plasmas. Motivated by the observed increase in ion temperature and SBS reflectivity measurements, we developed a model that includes trapping effects, providing the necessary saturation mechanism to give SBS reflectivity values consistent with the experiment.

The experiments used a three-beam configuration at the Trident Laser Facility [7]. The multi-ion-species targets consisted of a mixture of Be with 1%, 5%, or 10% Au by atomic number which was fabricated by coating a substrate with alternating Au-Be layers of varying thickness [8]. The plasma was produced by a heater beam with 180 J of 2ω ($\lambda = 527$ nm) laser light in a 1.2-ns-long square pulse. The heater beam was focused normal to the target surface (Fig. 1a) using an $f/6$ lens and a strip line random phase plate. This produced a line focus ($\sim 1000 \times 100$ μm) with an intensity of 10^{14} W cm^{-2} [9]. The targets were cut such that initially an 800×100 μm plasma was formed. A separate high energy 2ω interaction

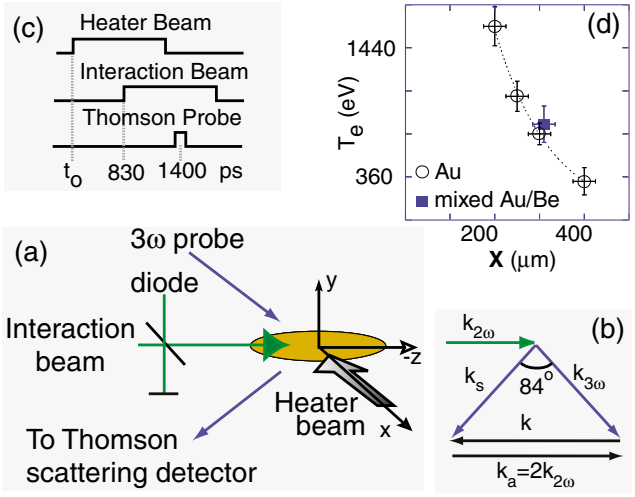

FIG. 1 (color). (a) Schematic of the experimental setup. (b) The angle between the incident ($\mathbf{k}_{3\omega}$) and scattered ($\mathbf{k}_s$) Thomson beam ($|k_{3\omega}| \simeq |k_s|$) is determined by matching the driven ion-wave vector ($\mathbf{k}_a \approx 2\mathbf{k}_{2\omega}$) with the Thomson-scattering wave vector ($\mathbf{k}$). (c) Relative beam timings. (d) The electron temperature is plotted as a function of the distance from the target surface at a time of 1.4 ns.

beam, 1.2-ns-long square pulse, was aligned parallel to the target and focused to a ~60 μm diameter spot, resulting in laser intensities up to 4×10^{15} W cm^{-2} [10]. The interaction beam was used to drive SBS which excites ion-acoustic waves in the plasma. The wave number of the excited ion-acoustic wave was matched using a third 3ω ($\lambda = 351$ nm) 180 ps Thomson-scattering probe beam (Fig. 1b). The beams were timed such that the interaction beam turned on 830 ps after the heater beam. The Thomson-scattering probe began 200 ps after the end of the heater beam (Fig. 1c). A region of plasma overlapping the interaction beam path was imaged onto a half-meter spectrometer with an optical magnification of 5:1. The cylindrical Thomson-scattering volume, centered in the y-z plane, was 60 μm long and 40 μm in diameter. The spectrally resolved Thomson-scattering signal was detected with a streak camera, resulting in a spectral and temporal resolution of 0.05 nm and 100 ps, respectively.

Figure 2 shows the Thomson-scattering data with and without the interaction beam at a distance of $x = 300$ μm from the target surface. The blow-off plasma was well characterized by fitting the standard multi-ion-species form factor [11,12] to the Thomson-scattering spectra taken in the absence of the interaction beam. The electron temperature, $T_e(x = 300) = 600$ eV, is directly determined by the separation of the fast Be-like mode since the Be ions are fully ionized, $Z_{\mathrm{Be}} = 4$. Furthermore, the phase velocity of the slow mode is sensitive to the product of the average Au charge state and electron temperature, $Z_{\mathrm{Au}}T_e$, therefore allowing the accurate measure of the charge state, $Z_{\mathrm{Au}}(x = 300) = 40$. The relative amplitude of the peaks in the Thomson scattering spectra belonging to the slow and fast ion-acoustic waves provides an accurate measure of the ion temperature, $T_i(x = 300) = 250$ eV. The product of the Au charge state and electron temperature, $Z_{\mathrm{Au}}T_e$, is measured along the heater beam

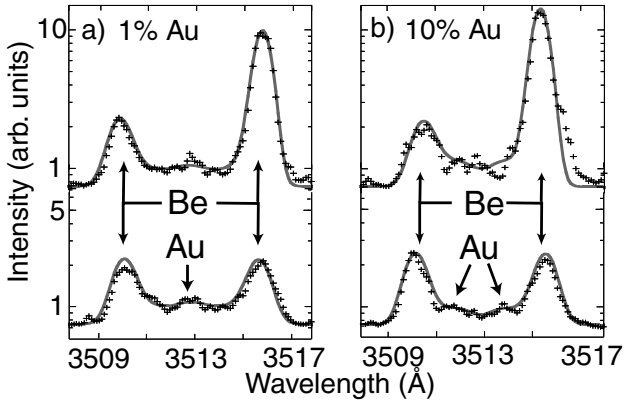

FIG. 2. The measured Thomson-scattering spectra (+) from Be plasmas with (a) 1% and (b) 10% Au. The solid line is the best fit theoretical form factor with the addition of a Gaussian line profile in the upper two plots. The bottom data set represents scattering when the interaction beam is turned off, while the upper spectra show data with an interaction beam intensity of 3.5×10^{15} W cm^{-2}.

axis by varying the distance of the Thomson-scattering volume from the Au disk targets (Fig. 1d). The average Au charge state was assumed to vary slowly from 43 at $x = 200$ μm to 38 at $x = 400$ μm [13].

The wavelength of the probe laser ($\lambda = 351$ nm), the scattering geometry, and the plasma parameters result in collective Thomson scattering from fluctuations characterized by wave numbers such that the scattering parameter is greater than one, $\alpha = 1/k\lambda_D \approx 3$, where k is the thermal Thomson-scattering wave vector and λ_D is the electron Debye length. An electron density of $n_e \simeq 10^{20}$ cm^{-3} was calculated by radiation-hydrodynamic modeling and is consistent with other experiments [14]. The collective ion effects are seen in Fig. 2, where representative scattering spectra are shown with two different ion concentrations revealing both the slow and the fast modes.

When the interaction beam is used, ion-acoustic waves are excited by SBS which produce backward scattered light. In order to measure the amplitude of the excited ion waves, the angle θ between the incident and scattered wave vectors of the Thomson-scattering probe was adjusted to match the Thomson-scattering wave vector, $k \simeq 2k_{3\omega} \sin\theta/2$ with the driven ion-wave vector $k_a \simeq 2k_{2\omega}$ giving $\theta = 84°$ (Fig. 1b). It is noted that we observe thermal ion-acoustic wave fluctuations in all the Thomson spectra, driven or undriven, as the blueshifted peaks.

The top spectra in Fig. 2 show that, once the interaction beam is turned on, only the redshifted peak belonging to the fast Be-like mode are excited by SBS. No excitation of the slow ion-acoustic wave has been observed. The spectra are fit using the standard theoretical form factor; when SBS is excited, a Gaussian line profile centered on the frequency of the fast Be-like peak is added. The area under the Gaussian line profile is varied to fit the driven peak. In the parameter regime of this experiment, the spatial growth of SBS from either acoustic mode is inversely proportional to its Landau damping. Because of the fast energy equilibration time between the Be and Au, we can assume each species has the same ion temperature. The solution to the multi-ion-species dispersion relation shows that the fast mode is weakly damped (the normalized Landau damping is $\nu_L/\omega_a = 0.05$ for a 10% Au mixture with $T_i/T_e \approx 0.3$) and the slow mode is heavily damped ($\nu_L/\omega_a = 0.3$). Our SBS linear gain calculations, using the codes LIP/PIRANAH [15], reproduce the findings of Fig. 2 with almost no amplification of the slow mode ($G_{\mathrm{SBS}} \approx 5$) and a large amplification for the fast mode ($G_{\mathrm{SBS}} \approx 200$).

Figure 3 shows the measured SBS reflectivity for various mixtures of Au and Be. These measurements have been performed by collecting and collimating the SBS light using the $f/6$ aspheric lens that focuses the interaction beam. The light is then reflected off a beam splitter, passed through a narrow 532 nm notch filter, and focused onto a diode that measured both the incident and backreflected SBS light (Fig. 1a). We observe the SBS reflectivity to be a few percent, while linear theory (i.e., convective gain)

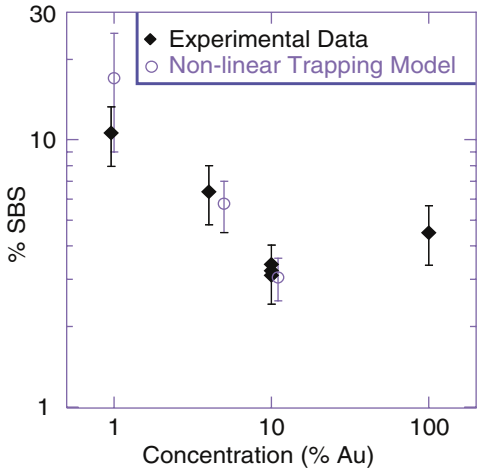

FIG. 3 (color). The SBS reflectivity has been measured to decrease for beryllium plasmas with increasing gold concentration (black diamonds). This trend is reproduced by our nonlinear trapping theory (blue circles).

gives a reflectivity of nearly 100%. It is therefore clear that, while our linear theory predicts the growth of the fast mode and not the slow mode as seen in Fig. 2, the SBS reflectivity data indicate a need for a nonlinear model that includes saturation of ion-acoustic waves.

Figure 4a shows the ion temperature increase as a function of the SBS excited ion-acoustic wave amplitude. The ion-wave amplitude is defined to be the square root of the ratio of the area under the redshifted spectra, to the area under the blueshifted spectra; the ion-wave amplitude is proportional to $\delta n/n_e$. Figure 4b indicates the sensitivity of the Thomson spectra to ion temperature. As the ion temperature increases, the damping of the fast mode increases while the damping of the slow mode decreases, resulting in a respective rise and fall in the blueshifted peaks of the thermal undriven Thomson spectra. With the interaction beam employed, the ion-wave amplitude increases and the ion temperature rises (Fig. 4a), while we found no change in the electron temperature. This direct observation of an increase in ion temperature indicates that ion trapping is important and could be the critical saturation mechanism.

In this experiment we excite ion-acoustic waves in the direction of the interaction beam. These driven ion waves trap ions which are accelerated (creating hot ions) in the same direction as the driven acoustic wave. After thermalization this will increase the average ion temperature which we measure from the blueshifted peaks in the Thomson-scattering spectrum; note that the blueshifted peaks result from scattering off ion-acoustic wave fluctuations in the direction counterpropagating to the original hot ions. We have therefore included these trapping effects in our nonlinear theory of SBS.

In our range of experimental parameters, $6 < Z_{\mathrm{Be}}T_e/T_i < 14$, the population of Be ions near the phase velocity of the ion-acoustic wave is large enough so that trapping effects are a plausible saturation mechanism. Trapping reduces the ionic part of the linear Landau

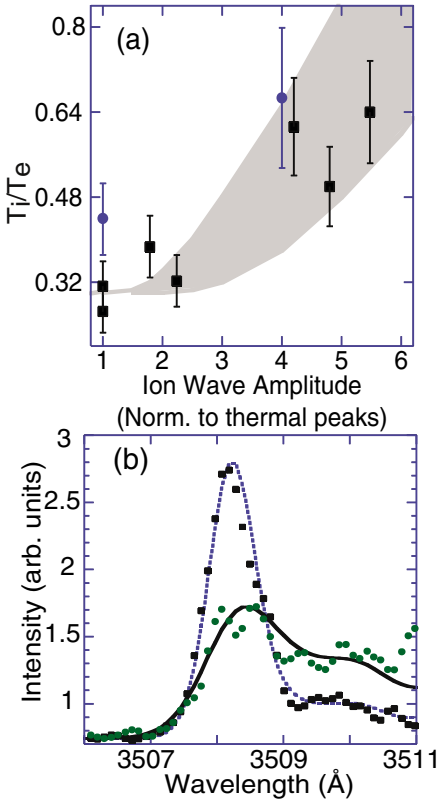

FIG. 4 (color). (a) The ratio of T_i/T_e as a function of ion-wave amplitude is plotted indicating hot ions and ion trapping. Data for Be with 5% Au (blue circles) and 10% Au (black squares) are shown. The solid green line is the result of modeling and shows good agreement with the experiment. (b) The blueshifted (thermal) Thomson-scattering spectra for a 10% Au mixture are shown for a shot without the interaction beam (black squares) and a shot with an interaction beam intensity of 3.5×10^{15} W cm^{-2} (green circles) resulting in an increase in ion temperature from 250 to 475 eV.

damping of the driven wave by flattening the distribution function around the phase velocity of the wave [5,16]; therefore, a lower limit for the residual damping, ν, is the electronic Landau damping and a small collisional damping ($\nu/\omega_s \approx 0.015$).

Another effect of the trapping is a modification of the dispersion relation for the SBS acoustic wave, creating a nonlinear frequency shift, $\delta\Omega$ [5,17,18]:

$$\frac{\delta\Omega}{\omega} \approx -\eta\left(\frac{\delta n}{n_e}\right)^{1/2} \equiv -\frac{f_{\mathrm{Be}}}{\sqrt{2\pi}}(v^4 - v^2)e^{-v^2/2}\sqrt{Z_{\mathrm{Be}}\frac{T_e}{T_i}}\left(\frac{\delta n}{n_e}\right)^{1/2}, \quad (1)$$

where η is the detuning parameter, ω_a is the SBS acoustic wave frequency, f_{Be} is the fraction of Be ions in the plasma ($f_{\mathrm{Be}} = 0.9$) , and $v = v_\phi/v_{\mathrm{Be}}$, $v_{\mathrm{Be}} = \sqrt{\frac{T_i}{M_{Be}}}$ is the thermal velocity of the Be ions. The phase velocity (v_ϕ) of the fast mode is given by the multi-ion-species dispersion relation (v^2 is of order of $Z_{\mathrm{Be}}T_e/T_i$). This nonlinear

frequency shift detunes the resonant coupling between the interaction beam and the ion-acoustic wave, therefore saturating the SBS instability.

Including these effects in a steady-state coupled-wave model of SBS gives (from Ref. [19]):

$$c\sqrt{1-\frac{n_e}{n_c}}\,\partial_z A_1(z) = -\frac{i\omega_0}{4}\,\frac{\delta n(z)^*}{n_e}\,\frac{n_e}{n_c}\,A_0\,, \qquad (2)$$

$$\left(i\eta\sqrt{\frac{\delta n}{n_e}}+\nu\right)\frac{\delta n(z)}{n_e} = \frac{i\omega_0^2}{\omega_a}\,\frac{Z_{\mathrm{Be}}m_e}{m_i}\left(\frac{v_0}{c}\right)^2\frac{A_1(z)^*}{A_0}\,, \qquad (3)$$

where A_0 (A_1) is the incoming (reflected) laser light vector potentials, ω_0 is the laser frequency, and v_0 is the electron quiver velocity. Balancing the two terms on the left-hand side of Eq. (3) shows that detuning becomes important for SBS saturation when $\delta n/n_e \approx \nu^2/\eta^2 \simeq 0.1\%$ for our parameters. The SBS reflectivity is calculated by integrating the system of equations [Eqs. (2) and (3)] between $z = 0$ and $z = L$ for different fractions of Au and is in rough agreement with the experimental values (Fig. 3). Parameters used in the model were selected to match the experiment (L = 800 μm, $T_i/T_e \approx 1/2$, $I_0 = 3\times10^{15}$ W cm^{-2}, $n_e = 10^{20}$ cm^{-3}). This model is dependent on the electron density and the interaction beam intensity; the error bars in Fig. 3 result from uncertainties in these experimental parameters. The scaling with the fraction of Au ions is well reproduced, and is mainly from a decreasing phase velocity of the fast mode when the fraction of Au ions is increased, which increases the number of ions at the phase velocity resulting in a larger detuning parameter (η) and therefore more efficient detuning, (i.e., the same acoustic wave amplitude creates a larger frequency shift).

We further test this model by estimating the ion temperature in the Thomson-scattering volume ($z = L/2$). We balance the energy flux deposited into the acoustic waves (from the Manley-Rowe relations) with a free streaming heat flux [20]:

$$\frac{\omega_s}{\omega_0}\,(R_{\mathrm{SBS}}I_0) \;=\; n_{\mathrm{Be}}T_i v_{\mathrm{Be}}\,. \qquad (4)$$

This model assumes that the energy deposition is local, i.e., the mean-free path of the hot ions accelerated by trapping (a few tens of μm) is much smaller than the length of the plasma ($L \approx 1$ mm), and thermalization is fast enough so that heat is carried away by Maxwellian ions when a steady state is reached. Theoretical and experimental ion-wave amplitudes were related by matching a high reflectivity point; the model then reproduces the experimental scaling for T_i. The gray area in Fig. 4a is due to the error in the modeled SBS reflectivity and the uncertainties in the energy loss to the electrons and Au ions.

Validation of the main assumptions of this modeling (a steady state is reached and the nonlinear frequency shift is the main effect that detunes and saturates the instability) through comparisons of particle-in-cell and fluid simulations is beyond the scope of this paper, but such a detuning effect has been emphasized in various publications [1,3,21]. The saturation mechanism governed by detuning will be much weaker in high-Z plasmas (CO2, pure Au) because the detuning parameter is a strong function of charge state.

In summary, we have presented the first measurements of the growth of ion-acoustic waves in well-characterized multi-ion-species plasmas. Our measurements of the SBS reflectivity indicate the need for a saturation mechanism. Using Thomson scattering and by adding a small fraction of Au ions to a Be plasma enabled the first accurate measurement of T_i in laser-plasma interaction studies; while T_i was found to increase with SBS reflectivity and with the amplitude of the (local) acoustic waves, T_e was found to be constant. This is consistent with our model, where the increase in T_i is due to trapping of ions by the SBS ion-acoustic waves.

We would like to acknowledge the efforts of the Trident laser crew: R. Johnson, T. Hurry, R. Gonzales, N. Okamoto, F. Archulata, S. Letzring, and R. Perea. We thank D. Montgomery, C. Labaune, E. Williams, B. Cohen, R. Berger, and H. Baldis for valuable discussions. We further thank R. Scalettar and the UC Davis Physics Department for their support. This work was performed under the auspices of the U.S. Department of Energy by the Lawrence Livermore National Laboratory under Contract No. W-7405-ENG-48.

*Also at Physics Department, University of California at Davis, California 95616.

[1] C. E. Clayton *et al.,* Phys. Rev. Lett. **51**, 1656 (1983).
[2] B. Gellert and B. Kronast, Appl. Phys. B **32**, 175 (1983).
[3] S. C. Wilks *et al.,* Phys. Rev. Lett. **74**, 5048 (1995).
[4] S. H. Glenzer *et al.,* Phys. Rev. Lett. **86**, 2565 (2000).
[5] B. I. Cohen *et al.,* Phys. Plasmas **4**, 956 (1997).
[6] E. A. Williams *et al.,* Phys. Plasmas **2**, 129 (1995).
[7] N. K. Moncur *et al.,* Appl. Opt. **34**, 4274 (1995).
[8] S. H. Glenzer *et al.,* Phys. Rev. Lett. **77**, 1496 (1996).
[9] B. S. Bauer *et al.,* Phys. Rev. Lett. **74**, 3604 (1995).
[10] R. P. Johnson (private communication).
[11] J. A. Fejer, Can. J. Phys. **38**, 1114 (1960).
[12] D. E. Evans, Plasma Phys. **12**, 573 (1970).
[13] M. E. Foord *et al.,* Phys. Rev. Lett. **85**, 992 (2000).
[14] D. S. Montgomery *et al.,* Phys. Rev. Lett. **84**, 678 (2000).
[15] L. V. Powers *et al.,* Phys. Plasmas **2**, 2473 (1995).
[16] V. E. Zakharov and V. I. Karpman, Sov. Phys. JETP **16**, 351 (1962).
[17] G. J. Morales and T. M. O'Neil, Phys. Rev. Lett. **28**, 417 (1972).
[18] A. A. Andreev and V. T. Tikhonchuk, JETP **68**, 1135 (1989).
[19] E. A. Williams and B. I. Cohen, in Proceedings of the APS-DPP01, Long Beach, CA, 2001, p. QP1.146.
[20] W. L. Kruer, Phys. Fluids **23**, 1273 (1980).
[21] H. X. Vu *et al.,* Phys. Rev. Lett. **86**, 4306 (2001).